Journal of Applied Physics ARTICLE scitation.org/journal/jap

Pressure-induced spin crossover in a $Fe_{78}Si_9B_{13}$ metallic glass

Cite as: J. Appl. Phys. **129**, 165901 (2021); doi: 10.1063/5.0050830
Submitted: 19 March 2021 · Accepted: 10 April 2021 ·
Published Online: 22 April 2021

Tao Liang,[1,2] Fei Zhang,[2,3] Xin Zhang,[2] Xiehang Chen,[2] Songyi Chen,[2] Hongbo Lou,[2] Zhidan Zeng,[2] Dazhe Xu,[2] Ke Yang,[4] Yuming Xiao,[5] Paul Chow,[5] Baolong Shen,[1] and Qiaoshi Zeng[1,2,a)]

AFFILIATIONS

[1]Jiangsu Key Laboratory of Advanced Metallic Materials, School of Materials Science and Engineering, Southeast University, Nanjing 211189, People's Republic of China
[2]Center for High Pressure Science and Technology Advanced Research, Pudong, Shanghai 201203, People's Republic of China
[3]China Spallation Neutron Source, Institute of High Energy Physics, Chinese Academy of Sciences, Dongguan 523000, People's Republic of China
[4]Shanghai Synchrotron Radiation Facility, Shanghai Advanced Research Institute (Zhangjiang Laboratory), Chinese Academy of Sciences, Shanghai, 201204, People's Republic of China
[5]HPCAT, X-ray Science Division, Argonne National Laboratory, Argonne, Illinois 60439, USA

[a)]**Author to whom correspondence should be addressed:** zengqs@hpstar.ac.cn

ABSTRACT

The pressure effect on structures and properties of a $Fe_{78}Si_9B_{13}$ metallic glass was investigated by *in situ* high-pressure synchrotron Fe $K\beta$ x-ray emission spectroscopy and x-ray diffraction, and electrical resistivity measurements up to ~51 GPa. The study reveals a reversible and continuous pressure-induced high- to low-spin crossover of Fe atoms in an amorphous structure. The changes of the local spin moment can be scaled to match its average atomic distance shrinkage very well during compression. The crossover of electronic spin states in the $Fe_{78}Si_9B_{13}$ metallic glass resembles that of typical crystalline Fe-bearing materials but without a sharp atomic volume collapse and an abrupt electrical resistivity jump. These findings could help guide applications of Fe-based metallic glasses as a soft ferromagnetic material at extreme conditions and also improve our understanding of magnetism and coupling of its changes with disordered atomic structures and other properties in metallic glasses.

I. INTRODUCTION

Due to the combination of highly disordered atomic structure and metallic bonding, metallic glasses (MGs) set themselves away from both conventional metallic alloys and network glasses with many unique properties,[1] e.g., MGs have mechanical strength close to theoretical values, high hardness and wear resistance, and excellent soft magnetic properties.[2,3] Besides their superior properties for widespread potential applications, MGs also provide a valuable model system for fundamental studies of glasses in general. Unlike the intuitive idea that MGs are randomly packed hard-sphere systems, the electronic interaction between different atoms is found to play an essential role in controlling the structures and properties of multicomponent MGs.[4–6] The electronic structure of MGs could be inherited from their crystalline counterparts. Therefore, in analogy to various polymorphic transitions in crystalline materials, interesting amorphous-to-amorphous, namely, polyamorphic phase transitions with electronic mechanism, were discovered in some MGs under high pressure.[7–10] These previous discoveries highlight the electronic effect on the disordered atomic structures and even possible structural transitions in MGs. It is well known that the magnetism of materials is closely associated with electronic structures and their interactions. Therefore, magnetic transitions could also have strong interactions with structures of materials. For example, magnetism is shown to be the primary stabilizing factor of the α phase of crystalline iron. The α–ϵ phase transition of iron can be well described within the fluctuation spin theory,[11] showing strong magneto-volume coupling.[12] In some iron-based alloys, magnetic fluctuation also accounts for their unusual Invar effect, in

which magneto-volume coupling also plays a key role.[13] Magnetic properties of MGs mainly depend on their local structure rather than long-range structural order.[14] The local structures in MGs and their crystalline counterparts could be similar to some extent.[15,16] Therefore, it is intriguing to ask whether the magnetic transitions often observed in crystalline materials might also be possible with disordered atomic structures in MGs, resulting in tunable properties and structures or even polyamorphism transitions in MGs.

Exploration of properties of materials at extreme conditions is not only meaningful to practical applications but also could uncover novel phenomena and shed new light on long-standing fundamental questions. High pressure is powerful in tuning atomic, electronic, and also magnetic structures of materials over a wide range.[17,18] X-ray emission spectroscopy (XES) is a well-established technique that allows direct detection of the local magnetic moment of selected elements in various environments without reference to the long-range magnetic order. Although the x-ray circular magnetic dichroism (XMCD) and Mössbauer spectroscopy (MS) are also element selective probes, they reply on the long-range magnetic order. Therefore, XMCD and MS could not distinguish a paramagnetic state from a diamagnetic state, for example, a pressure-induced reduction of Curie temperature from a true reduction of local magnetic moment on individual atoms. By employing *in situ* high-pressure XES as a sensitive probe,[19] pressure-induced magnetic transitions between high-spin and low-spin electronic states were extensively reported in crystalline Fe,[12,20,21] Fe-based alloys,[13,22] and Fe-bearing compounds.[23–28] Basically, high enough pressure triggers spin-pairing transitions of the 3*d* electrons in Fe due to changes of crystal field splitting or electron band widening,[29] which could be clearly manifested as reduction or disappearance of the satellite intensity in the Fe $K\beta$ XES emission line.[30] Accompanying the spin transitions, there are usually resultant discontinuous changes of properties and atomic structural phase transitions with atomic volume collapse during compressing of various crystalline materials and minerals.[31–35] However, whether similar spin transitions exist in amorphous materials and how the disordered atomic structure and properties will be affected have not been well explored.[36] In this work, *in situ* high-pressure synchrotron Fe $K\beta$ XES combined with x-ray diffraction (XRD) and four-probe electrical resistance measurements were carried out on a prototype $Fe_{78}Si_9B_{13}$ MG up to 51 GPa in a diamond anvil cell (DAC). An interesting reversible spin crossover was observed in the $Fe_{78}Si_9B_{13}$ MG, and its coupling with the average atomic distance and properties as a function of pressure was discussed.

II. EXPERIMENTAL

Fe-based MGs have been used as soft magnetic materials in industry because of their high permeability and low coercivity.[37] Among them, $Fe_{78}Si_9B_{13}$ is a prototype soft ferromagnetic MG (Curie temperature at ~680 K), which has attracted much attention due to its good glass-forming ability and superior performance parameters.[38] More interestingly, the $Fe_{78}Si_9B_{13}$ MG was reported to show the Invar effect.[39] Therefore, the $Fe_{78}Si_9B_{13}$ MG was chosen as a model system in this study. Master ingots with a nominal composition of $Fe_{78}Si_9B_{13}$ were prepared by melting pure Fe (99.99 wt. %), Si (99.99 wt. %), and B (99.999 wt. %) in an arc-melting device under a Ti-gettered high-purity Ar atmosphere. Ingots were flipped and re-melted at least five times to ensure their compositional homogeneity. $Fe_{78}Si_9B_{13}$ MG ribbons with a thickness of ~30 μm and a width of ~2 mm were further fabricated from the master ingots using a single roller melt-spinning technique. The glass nature of prepared $Fe_{78}Si_9B_{13}$ MG ribbons was verified by in house XRD and differential scanning calorimetry (DSC).

In situ high-pressure XES measurements were carried out at the beamline 16-IDD, High Pressure Collaborative Access Team (HPCAT) at the Advanced Photon Source (APS), Argonne National Laboratory (ANL), USA. The sample chamber was a hole with a diameter of ~150 μm drilled in the center of a pre-indented indent of an x-ray transparent beryllium (Be) gasket. A piece of $Fe_{78}Si_9B_{13}$ ribbon was cut into an approximately $50 \times 50 \times 25\ \mu m^3$ chip. It was then loaded into a Mao-type symmetric DAC along with a tiny ruby ball beside the sample as a pressure calibrant. The pressure-transmitting medium was silicone oil. A micro-focused x-ray beam (~$11 \times 10\ \mu m^2$) went through one of the diamond anvils to shine on the sample, while the emitted Fe $K\beta$ x ray passing through the Be gasket with directions perpendicular to the incident x-ray beam was collected.[19] By taking into account the undulator flux and the diamond anvil absorption, the incident x-ray energy was set to 11.6 keV. The x-ray energy was calibrated by measuring the Fe $K\beta$ spectrum of a standard pure Fe foil and then setting the peak energy to tabulated Fe $K\beta_{1,3}$ peak energy at 7058 eV. Fe $K\beta$ spectra were acquired by scanning a bent Si analyzer with a step of 0.4 eV from 7017 to 7083 eV. The exposure time for each energy point was 25 s.

In situ high-pressure XRD experiments with an x-ray wavelength of 0.6199 Å and a focused beam size of ~$4 \times 10\ \mu m^2$ were performed at the beamline 15U1, Shanghai Synchrotron Radiation Facility (SSRF), China. The sample loading method was the same as the *in situ* high-pressure XES experiments, but a rhenium (Re) gasket was used instead of Be. The 4:1 (volume ratio) mixture of methanol–ethanol was loaded in the DAC as the pressure-transmitting medium.

The standard four-probe method was employed for *in situ* high-pressure electrical resistance measurements using a cross DAC with an anvil culet size of ~400 μm. A T301 stainless steel gasket was pre-indented to ~20 GPa, and a hole of ~380 μm was drilled inside the indent. Then the hole was re-filled with a mixture of epoxy and cubic-BN (cBN), which was compressed to ~20 GPa again to reliably insulate the electrodes and sample against the steel gasket to target pressures. A hole of ~150 μm was drilled again at the center of the epoxy + cBN indent as the sample chamber and then filled with NaCl as the pressure-transmitting medium. A $Fe_{78}Si_9B_{13}$ ribbon sample was cut into a rectangle shape with a size of ~$130 \times 50\ \mu m^2$ by focused ion beam (FEI Versa 3D) and placed on the NaCl. Four electrodes made of Pt thin foil (~4 μm in thickness) were implanted for the current source and voltage measurement. A constant current of 20 mA was supplied by a DC current source (Keithley-6221), and the voltage was monitored by a nanovoltmeter (Keithley-2182A).

III. RESULTS AND DISCUSSION

In situ high-pressure XES was carried out on the $Fe_{78}Si_9B_{13}$ MG to monitor the spin state and its evolution during compression and decompression at room temperature (Fig. 2). To present the

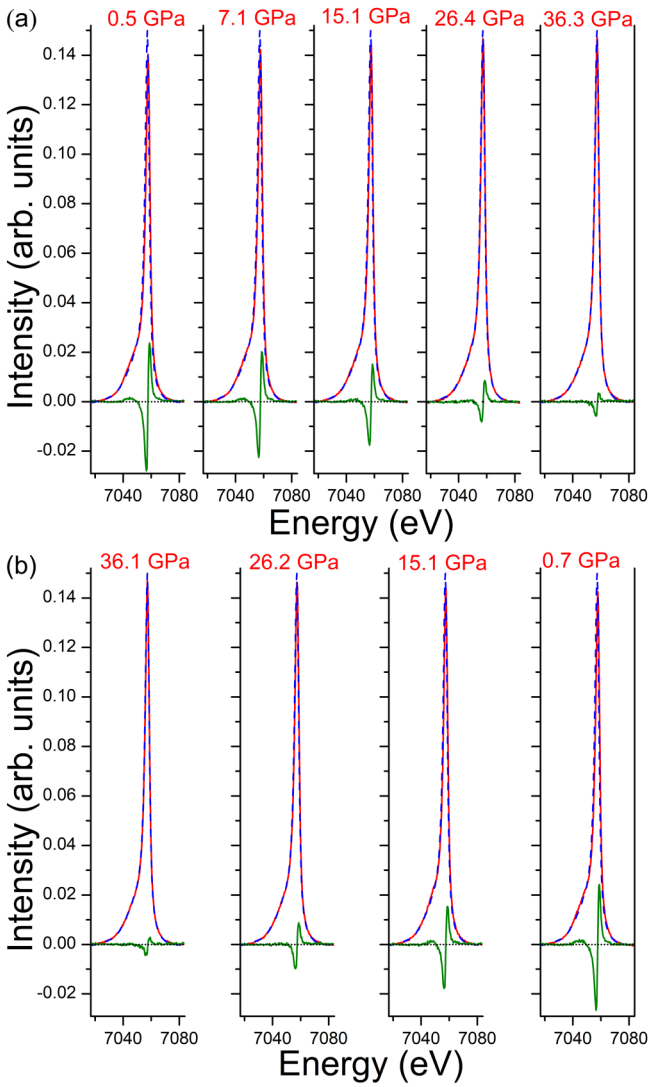

FIG. 1. Fe $K\beta$ XES spectra of the $Fe_{78}Si_9B_{13}$ MG at room temperature during compression (a) and decompression (b). Green solid lines are the difference spectra, which are obtained by subtracting the XES spectra (solid red lines) from the highest-pressure spectrum at 50.5 GPa (blue dashed lines). The horizontal black dotted lines mark the difference value of zero.

small changes of the local magnetic moment from the $K\beta$ line profile, each spectrum is normalized to the unit area at integral and compared with the highest-pressure spectrum at ~50.5 GPa as a reference for subtraction.[30] The shoulder associated with the $K\beta'$ satellite is revealed by asymmetry at the low-energy side of the primary peak. According to the difference spectra, with increasing pressure, the difference continuously decreases to the highest pressure. A shift to the lower energy of the primary peak ($K\beta_{1,3}$ at ~7058 eV) and loss of spectral weight in the $K\beta'$ regions around 7045 eV can be observed during compression by the difference

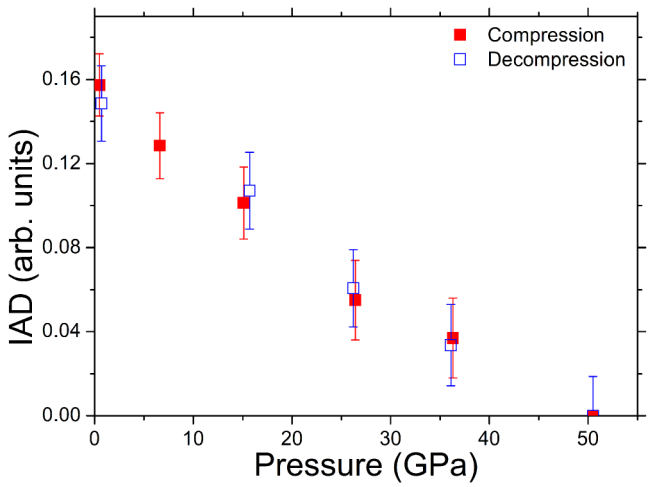

FIG. 2. The pressure-dependent IAD values of Fe local spin moment in the $Fe_{78}Si_9B_{13}$ MG. The IAD values change continuously and reversibly during compression (solid red squares) and decompression (open blue squares) over the entire pressure range.

spectra, indicating a reduction of the spin moment of Fe with increasing pressure [Fig. 2(a)]. A clearer comparison of the $K\beta'$ satellite intensities during compression can be found in Fig. S1 in the supplementary material. During decompression, the difference between the high-pressure spectra and reference spectrum increases again, and the intensity almost recovers to the initial values when the pressure is released, which indicates a reversible spin crossover from low-spin back to high-spin in Fe [Fig. 2(b)].[12] Without a careful comparison with a reference spectrum of a known material with similar coordination environment and the same experimental conditions, it is not clear about the absolute value of the local spin moment of the sample at ~50.5 GPa. However, the spectrum at ~50.5 GPa could still provide a good reference to estimate the relative change of the spin states toward the lower spin state and the electronic structure stabilities during compression.

To track the variation of the spin state quantitatively, the integrals of the absolute values of the difference (IAD) spectra can be used, which are proportional to the spin magnetic moment of Fe atoms.[30] After all spectra are normalized to the unit area at integration, the IAD value for any spectrum SP_i with respect to a reference spectrum SP_{ref} is obtained as a numerical approximation to Eq. (1),

$$IAD_i = \int_{E1}^{E2} |SP_i - SP_{ref}| dE, \quad (1)$$

where $E1$ and $E2$ are the lower and upper limits of the energy for XES spectra. IAD values have been proved to be a reliable quantitative measure for the rapid determination of spin states from XES spectra, especially when dealing with weak moments.[30] Since high pressure is known to suppress the local magnetic moments as observed in many Fe-bearing materials,[12] we use the spectrum at 50.5 GPa as a reference of relative low-spin state to track the extent

of spin crossover. The IAD value is set to be zero at 50.5 GPa, which defines the relatively lowest spin state achieved in this experiment. The change of IAD values as a function of pressure during compression and decompression indicates that the pressure-induced spin reduction is continuous and reversible in the $Fe_{78}Si_9B_{13}$ MG (Fig. 3). Moreover, the reduction starts once pressure is applied. However, the spin reduction seems still far from completion according to the lack of any plateau up to the highest pressure of 50.5 GPa in this study, which is different from the commonly observed relative sharp spin transitions with two plateau zones before and after in many Fe-bearing crystalline materials.[12,20–22,40] Relative sluggish spin transitions were also reported in some Fe-bearing compounds due to their random Fe ion environments (chemical disorder).[35,41,42]

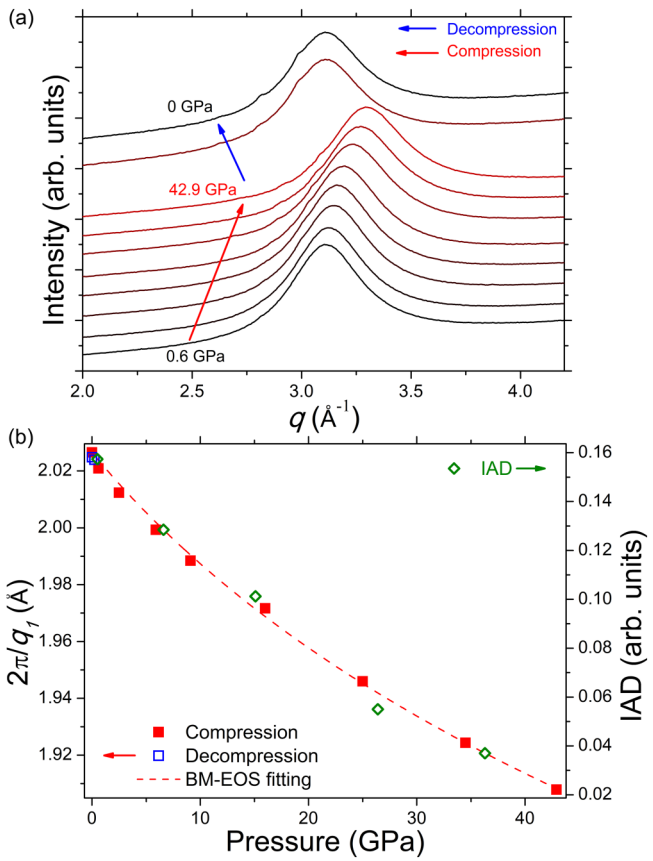

FIG. 3. Structural evolution and its interplay with spin crossover in the $Fe_{78}Si_9B_{13}$ MG. (a) *In situ* high-pressure XRD patterns of the $Fe_{78}Si_9B_{13}$ MG during compression from ~0.6 to ~42.9 GPa and decompression to ambient pressure. The small sharp peaks on the amorphous signal during compression are from the stainless steel gasket due to the sample chamber shrinkage. (b) Comparison of the inverse principal diffraction peak position, $2\pi/q_1$ (compression: solid red squares, decompression: open blue squares; error bars are smaller than the symbol size) and IAD values during compression (open green diamonds) with a linear scaling. The red dashed line fits the $2\pi/q_1$ vs pressure data by the second-order BM-EOS, which yields a bulk modulus $B_0 = 162.5 \pm 2.1$ GPa.

Therefore, the highly sluggish spin crossover over a broad range of pressure in the $Fe_{78}Si_9B_{13}$ MG could be associated with the highly diverse local environments of Fe atoms caused by its both chemically and topologically disordered atomic structure.[43] On the other hand, the structural heterogeneity[44] of MGs that is challenging to detect could be reflected by the sluggishness of this pressure-induced spin crossover. Although we cannot directly deduce the exact magnetic moment from the XES data, the high-spin to low-spin crossover implies that the macromagnetism of the $Fe_{78}Si_9B_{13}$ MG might be gradually suppressed by high pressure as well, which could affect the magnetic properties and magnetoelastic coupling with atomic structure.

In many crystalline Fe-bearing materials, pressure-induced high-spin to low-spin transition usually couples with apparent atomic volume collapse.[12,31,34] Therefore, it is necessary to check the volume change of the $Fe_{78}Si_9B_{13}$ MG (a non-crystalline form) accompanying the spin crossover during compression. Figure 4(a) shows the XRD patterns of the sample at different pressures during compression up to ~43 GPa and decompression to ambient conditions. With increasing pressure, the principal diffraction peak of the XRD pattern shifts toward the higher q direction, as expected for the densification effect of hydrostatic pressure. The sample remains fully amorphous over the entire pressure range, as indicated by the smooth patterns and absence of sharp Bragg peaks. In order to quantitatively track the shift of the principal diffraction peak, all the peaks are fitted using a Voigt line profile. Figure 4(b) shows the inverse principal peak position, $2\pi/q_1$, as a function of pressure, which is proved to be proportional to the average atomic distance, d, in MGs.[45] The smooth trend of $2\pi/q_1$ vs pressure suggests that there is no sharp first-order structural phase transition.[9]

It has been well established that the inverse diffraction peak position, $2\pi/q_1$, of a glass correlates with its volume, V, with a simple

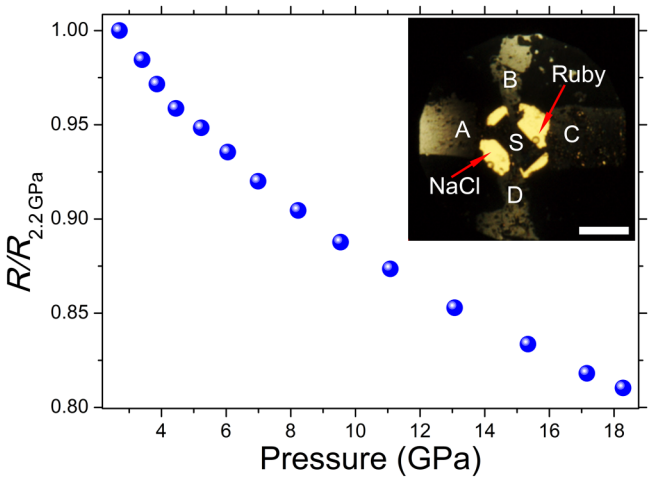

FIG. 4. Normalized resistance ($R/R_{0.2\,GPa}$) as a function of pressure of the $Fe_{78}Si_9B_{13}$ MG during compression up to ~18.3 GPa. The inset is an image of a rectangular sample (marked as S) loaded in a DAC with four Pt leads (A and D for the current supply) and (B and C for the voltage determination).

power law function,[46–48] e.g., $V \propto (2\pi/q_1)^3$. Hence, $2\pi/q_1$ can be conveniently used to estimate the relative volume (density) change of glass under pressure. $2\pi/q_1$ as a function of pressure of the $Fe_{78}Si_9B_{13}$ MG can be very well fitted by a second-order Birch–Murnaghan isothermal equation of state (BM-EOS) over the entire pressure range,[49] with an isothermal bulk modulus $B_0 = 162.5 \pm 2.1$ GPa and its pressure derivative B'_0 fixed at 4 if a 1/3 power law is employed [Fig. 4(b)]. This smooth change of the average atomic distance (volume) described by a single BM-EOS also confirms the absence of a relatively sharp amorphous-to-amorphous transition as observed in the previous polyamorphous MGs.[7–10] However, the bulk modulus obtained here by the BM-EOS fitting is smaller than the typical values (~180 to ~200 GPa) of Fe-based MGs with similar compositions.[50] This bulk modulus softening might be attributed to coupling between its magnetism and atomic structure of the $Fe_{78}Si_9B_{13}$ MG, i.e., a magneto-volume Invar effect as observed when heating the $Fe_{78}Si_9B_{13}$ MG.[39] This result is also similar to the observation of the magneto-volume effect in some chemically disordered high-entropy alloys, in which suppression of magnetism causes softening of the solid solution lattice.[51] In addition, surprisingly, the IAD values vs pressure could be linearly scaled to perfectly overlap with the average atomic distance shrinkage [Fig. 4(b)], which also supports coupling of the magnetic to elastic changes. The continuous and gradual structural and magnetic crossover in disordered magnetic alloys could be beneficial for applications that need to avoid an abrupt magneto-volume collapse.

Spin crossover usually also has a dramatic effect on other physical properties.[52] As a sensitive property to electronic, magnetic, and structural changes, electrical resistance as a function of pressure of the MG was further studied. In Fig. 1, the normalized change of electrical resistance ($R/R_{2.2\,GPa}$) shows a smooth and monotonic decrease with compression without any sharp jump or kink, which is consistent with the smooth reduction of the IAD values (local magnetic moment) and the average atomic distance shown in Fig. 4(b), confirming the continuous feature of the pressure-induced changes of the electronic and atomic structures in the $Fe_{78}Si_9B_{13}$ MG.

IV. CONCLUSION

In summary, a pressure-induced reversible continuous spin crossover was observed in the $Fe_{78}Si_9B_{13}$ MG by *in situ* high-pressure $K\beta$ XES. The spin crossover is sensitive to applying pressure but very sluggish without completion up to ~51 GPa. The atomic structure and sample volume (average atomic distance) monitored by *in situ* high-pressure XRD show continuous and reversible elastic densification under pressure as well; no obvious sharp structural transition is detected. Interestingly, the spin reduction could be linearly scaled to perfectly overlap with the average atomic distance shrinkage during compression. Moreover, the bulk modulus estimated by the BM-EOS fitting of the volume data is considerably smaller than that of the other MGs with similar compositions at ambient conditions. Therefore, we could speculate that the magnetic structure and behavior of crystalline materials may be inheritable to their glass counterparts, which could show a similar magneto-volume effect in MGs. Unlike the well-established theories in crystalline materials, the theories for magnetism in MGs are more phenomenological and based on assumptions.[14] Therefore, constraints from experiments are critical to deepening our understanding of the magnetic properties of MGs. The pressure effect on the Curie temperature and saturation magnetization has been extensively explored before and was correlated to the structural heterogeneity.[53,54] The sluggish spin crossover observed in this work more explicitly suggests a heterogeneous atomic structure in MGs. The findings in this work could deepen our understanding of magnetic properties of MGs, especially the inheritance between MGs and crystals based on the electronic mechanism. Meanwhile, it could also guide possible applications of ferromagnetic MGs under extreme conditions.

SUPPLEMENTARY MATERIAL

See the supplementary material for a clearer comparison of the $K\beta'$ satellite intensities in the XES spectra during compression.

ACKNOWLEDGMENTS

The authors thank Dr. Viktor V. Struzhkin, Professor Jung-Fu Lin, and Dr. Yang Ding for their helpful discussions and Dr. Yanping Yang for her assistance with sample cutting using FIB. This work was supported by the National Natural Science Foundation of China (Grant Nos. 51871054 and U1930401) and the Fundamental Research Funds for the Central Universities. The *in situ* high-pressure XES experiment was performed at the beamline 16-ID-D, HPCAT, Advanced Photon Source (APS), Argonne National Laboratory (ANL). HPCAT operations were supported by DOE-NNSA's Office of Experimental Sciences. The APS is a U.S. Department of Energy (DOE) Office of Science User Facility operated for the DOE Office of Science by ANL under Contract No. DE-AC02-06CH11357. The *in situ* high-pressure XRD experiment was performed at the beamline 15U1 at Shanghai Synchrotron Radiation Facility (SSRF), China.

DATA AVAILABILITY

The data that support the findings of this study are available from the corresponding author upon reasonable request.

REFERENCES

[1] A. L. Greer and E. Ma, MRS Bull. **32**, 611 (2007).
[2] W. H. Wang, Adv. Mater. **21**, 4524 (2009).
[3] M. F. Ashby and A. L. Greer, Scr. Mater. **54**, 321 (2006).
[4] Y. Q. Cheng, E. Ma, and H. W. Sheng, Phys. Rev. Lett. **102**, 245501 (2009).
[5] P. F. Guan, T. Fujita, A. Hirata, Y. H. Liu, and M. W. Chen, Phys. Rev. Lett. **108**, 175501 (2012).
[6] C. C. Yuan, F. Yang, X. K. Xi, C. L. Shi, D. Holland-Moritz, M. Z. Li, F. Hu, B. L. Shen, X. L. Wang, A. Meyer, and W. H. Wang, Mater. Today **32**, 26 (2020).
[7] H. W. Sheng, H. Z. Liu, Y. Q. Cheng, J. Wen, P. L. Lee, W. K. Luo, S. D. Shastri, and E. Ma, Nat. Mater. **6**, 192 (2007).
[8] Q. S. Zeng, Y. C. Li, C. M. Feng, P. Liermann, M. Somayazulu, G. Y. Shen, H. K. Mao, R. Yang, J. Liu, T. D. Hu, and J. Z. Jiang, Proc. Natl. Acad. Sci. U.S.A. **104**, 13565 (2007).
[9] Q. S. Zeng, Y. Ding, W. L. Mao, W. G. Yang, S. V. Sinogeikin, J. F. Shu, H. K. Mao, and J. Z. Jiang, Phys. Rev. Lett. **104**, 105702 (2010).
[10] G. Li, Y. Y. Wang, P. K. Liaw, Y. C. Li, and R. P. Liu, Phys. Rev. Lett. **109**, 125501 (2012).

[11]H. Hasegawa and D. G. Pettifor, Phys. Rev. Lett. **50**, 130 (1983).
[12]J. P. Rueff, M. Krisch, Y. Cai, A. Kaprolat, M. Hanfland, M. Lorenzen, C. Masciovecchio, R. Verbeni, and F. Sette, Phys. Rev. B **60**, 14510 (1999).
[13]M. van Schilfgaarde, I. A. Abrikosov, and B. Johansson, Nature **400**, 46 (1999).
[14]R. C. O'Handley, in *Amorphous Metallic Alloys*, edited by F. E. Luborsky (Butterworth-Heinemann, 1983), p. 257.
[15]H. W. Sheng, W. K. Luo, F. M. Alamgir, J. M. Bai, and E. Ma, Nature **439**, 419 (2006).
[16]Z. W. Wu, M. Z. Li, W. H. Wang, and K. X. Liu, Nat. Commun. **6**, 6035 (2015).
[17]H. K. Mao, B. Chen, J. Chen, K. Li, J. F. Lin, W. Yang, and H. Zheng, Matter Radiat. Extremes **1**, 59 (2016).
[18]M. Lesik, T. Plisson, L. Toraille, J. Renaud, F. Occelli, M. Schmidt, O. Salord, A. Delobbe, T. Debuisschert, and L. Rondin, Science **366**, 1359 (2019).
[19]Y. M. Xiao, P. Chow, and G. Y. Shen, High Pressure Res. **36**, 315 (2016).
[20]A. Monza, A. Meffre, F. Baudelet, J. P. Rueff, M. d'Astuto, P. Munsch, S. Huotari, S. Lachaize, B. Chaudret, and A. Shukla, Phys. Rev. Lett. **106**, 247201 (2011).
[21]B. W. Lebert, T. Gorni, M. Casula, S. Klotz, F. Baudelet, J. M. Ablett, T. C. Hansen, A. Juhin, A. Polian, and P. Munsch, Proc. Natl. Acad. Sci. U.S.A. **116**, 20280 (2019).
[22]J. P. Rueff, M. Krisch, and M. Lorenzen, High Pressure Res. **22**, 53 (2002).
[23]J. P. Rueff, C. C. Kao, V. V. Struzhkin, J. Badro, J. Shu, R. J. Hemley, and H. K. Mao, Phys. Rev. Lett. **82**, 3284 (1999).
[24]J. Badro, V. V. Struzhkin, J. F. Shu, R. Hemley, H. K. Mao, C. Kao, J. P. Rueff, and G. Y. Shen, Phys. Rev. Lett. **83**, 4101 (1999).
[25]J. Badro, G. Fiquet, F. Guyot, J.-P. Rueff, V. V. Struzhkin, G. Vankó, and G. Monaco, Science **300**, 789 (2003).
[26]J. F. Lin, V. V. Struzhkin, H. K. Mao, R. J. Hemley, P. Chow, M. Y. Hu, and J. Li, Phys. Rev. B **70**, 212405 (2004).
[27]J. Badro, J.-P. Rueff, G. Vankó, G. Monaco, G. Fiquet, and F. Guyot, Science **305**, 383 (2004).
[28]J. F. Lin, V. V. Struzhkin, S. D. Jacobsen, M. Y. Hu, P. Chow, J. Kung, H. Z. Liu, H. K. Mao, and R. Hemley, Nature **436**, 377 (2005).
[29]R. E. Cohen, I. I. Mazin, and D. G. Isaak, Science **275**, 654 (1997).
[30]G. Vankó, T. Neisius, G. Molnar, F. Renz, and F. M. F. Groot, J. Phys. Chem. B **110**, 11647 (2006).
[31]G. K. Rozenberg, M. P. Pasternak, W. M. Xu, L. S. Dubrovinsky, S. Carlson, and R. D. Taylor, EPL **71**, 228 (2005).
[32]A. F. Goncharov, V. V. Struzhkin, and S. D. Jacobsen, Science **312**, 1205 (2006).
[33]J. F. Lin, G. Vanko, S. D. Jacobsen, V. Lota, V. V. Struzhkin, V. B. Prakapenka, A. Kuznetsov, and C. S. J. S. Yoo, Science **317**, 1740 (2007).
[34]S. Javaid, M. J. Akhtar, I. Ahmad, M. Younas, S. H. Shah, and I. Ahmad, J. Appl. Phys. **114**, 243712 (2013).
[35]S. Layek, E. Greenberg, W. Xu, G. K. Rozenberg, M. P. Pasternak, J.-P. Itié, and D. G. Merkel, Phys. Rev. B **94**, 125129 (2016).
[36]Z. Mao, J. F. Lin, J. Yang, J. Wu, H. C. Watson, Y. M. Xiao, P. Chow, and J. Zhao, Am. Mineral. **99**, 415 (2014).
[37]H. X. Li, Z. C. Lu, S. L. Wang, Y. Wu, and Z. P. Lu, Prog. Mater. Sci. **103**, 235 (2019).
[38]L. L. Meng, X. Y. Li, J. Pang, L. Wang, B. An, L. J. Yin, K. K. Song, and W. M. Wang, Metall. Mater. Trans. A **44**, 5122 (2013).
[39]H. J. Ma, J. T. Zhang, G. H. Li, W. X. Zhang, and W. M. Wang, J. Alloys Compd. **501**, 227 (2010).
[40]J. P. Rueff, A. Mattila, J. Badro, G. Vankó, and A. Shukla, J. Phys.: Condens. Matter **17**, S717 (2005).
[41]I. S. Lyubutin, J. F. Lin, A. G. Gavriliuk, A. A. Mironovich, A. G. Ivanova, V. V. Roddatis, and A. L. Vasiliev, Am. Mineral. **98**, 1803 (2013).
[42]S. Speziale, A. Milner, V. E. Lee, S. M. Clark, M. P. Pasternak, and R. Jeanloz, Proc. Natl. Acad. Sci. U.S.A. **102**, 17918 (2005).
[43]J. Beille, A. Liénard, and J. P. Rebouillat, J. Phys. Colloq. **40**, 256 (1979).
[44]J. C. Qiao, Q. Wang, J. M. Pelletier, H. Kato, R. Casalini, D. Crespo, E. Pineda, Y. Yao, and Y. Yang, Prog. Mater. Sci. **104**, 250 (2019).
[45]H. F. Poulsen, J. A. Wert, J. Neuefeind, V. Honkimäki, and M. Daymond, Nat. Mater. **4**, 33 (2005).
[46]D. Ma, A. D. Stoica, and X. L. Wang, Nat. Mater. **8**, 30 (2009).
[47]A. R. Yavari, A. L. Moulec, A. Inoue, N. Nishiyama, N. Lupu, E. Matsubara, W. J. Botta, G. Vaughan, M. D. Michiel, and Å. Kvick, Acta Mater. **53**, 1611 (2005).
[48]Q. S. Zeng, Y. Kono, Y. Lin, Z. D. Zeng, J. Y. Wang, S. V. Sinogeikin, C. Park, Y. Meng, W. G. Yang, H. K. Mao, and W. L. Mao, Phys. Rev. Lett. **112**, 185502 (2014).
[49]F. Birch, J. Geophys. Res. **57**, 227, https://doi.org/10.1029/JZ057i002p00227 (1952).
[50]W. H. Wang, Prog. Mater. Sci. **57**, 487 (2012).
[51]L. Liu, S. Huang, L. Vitos, M. Dong, E. Bykova, D. Zhang, B. S. G. Almqvist, S. Ivanov, J.-E. Rubensson, B. Varga, L. K. Varga, and P. Lazor, Commun. Phys. **2**, 42 (2019).
[52]J. Badro, Annu. Rev. Earth Planet. Sci. **42**, 231 (2014).
[53]E. P. Wohlfarth, in *Amorphous Metallic Alloys*, edited by F. E. Luborsky (Butterworth-Heinemann, 1983), p. 283.
[54]L. F. Kiss, T. Kemény, J. Bednarčík, J. Gamcová, and H. P. Liermann, Phys. Rev. B **93**, 214424 (2016).